DECLASSIFIED
AUTH

IMAGE ANALYSIS STUDY OF THREE SAMPLES FROM A BASE-METAL ORE IN PORTUGAL

W. Petruk
Mineral Processing Laboratory

Project: 30.13.05
Liberation/Flotation Models
30.13.99
Cost Recovery

Job No: 025242

74 pp

MINERAL SCIENCES LABORATORIES
DIVISION REPORT MSL 87-11 (CR)

MICROMEDIA

CONFIDENTIAL

IMAGE ANALYSIS STUDY OF THREE SAMPLES FROM A BASE-METAL ORE IN PORTUGAL

by

W. Petruk

91-04949/

SUMMARY

Samples of a crushed pyrite ore, a pyrite sinter, and a chalcopyrite flotation tailing were analyzed by image analysis. The pyrite ore consists of large pieces, but the minerals are very fine grained. Most of the sphalerite, chalcopyrite and galena occur in interstices among pyrite grains, and the indicated minimum and optimum grinds for liberating and recovering the minerals are 80% minus 30 μm and 80% minus 13 μm respectively. The pyrite sinter consists of large hematite-magnetite pieces and contains a few small rounded spheres of Zn-Cu-Fe sulphates. The zinc and copper in the sinter occur mainly in the sulphates and magnetite, but minor proportions are in sphalerite and chalcopyrite remnants. The copper flotation tailing contains about 4.7 wt% chalcopyrite. The chalcopyrite is present as unliberated grains but 70% of the mineral is in particles that contain more than 60% chalcopyrite. Such particles are commonly recovered in copper concentrates.

Keywords: copper flotation-tailings, pyritic ore, sinter, pyrite chalcopyrite, sphalerite, hematite, sulphates

INTRODUCTION

Mr. Francisco Rodrigues of Laboratorio Nacional de Engenharia E Tecnologia Industrial (LNETI) of Lisboa, Portugal, enquired in January 1987 whether three samples of pyrite sinters could be analyzed as a cost recovery project to determine phase contents, size analyses, and mineral liberations. It was agreed that the work could be performed at an estimated cost of $1500. The samples arrived in June 1987, but could not be analyzed until September. The samples were labelled LSA-01-pyrite, LSA-02-pyrite cynders, and LSA-03- copper flotation tailings. The nature of the samples was found to be such that the reason for the analyses was not apparent. Consequently, it was assumed that (1) the pyrite sample was to be analyzed to predict the behaviour of the minerals during mineral beneficiation, (2) the sinter sample was to be analyzed to characterize the material and to determine the mode of occurrence of zinc and copper, and (3) the copper flotation tailing was to be analyzed to determine contents, size distributions, and liberation characteristics of the minerals. More work than anticipated was required in order to fulfill the assumed objectives. Even by extending the maximum time that could be allotted to the project the information that was obtained is the minimum that is needed for interpretations regarding mineral beneficiation and metallurgy.

RESULTS

LSA-01 (pyrite)

The sample was screened into plus 424 µm (+35 mesh), 424-53 µm (35-270 mesh) and minus 53 µm (-270 mesh) fractions because the size range of the particles was too wide for analysis in one polished section. The weight per cent of the fractions was: +424 µm 87.9, 424-53 µm 7.4, and -53 µm 4.7. Polished sections were prepared from the fractions and analyzed, with the MP-SEM-IPS image analysis system. The data were combined by computer by allocating the contribution of each fraction to the sample on the basis of weight per cent.

The minerals were identified with the energy dispersive X-ray analyzer (EDXA), and the areal fractions of the minerals in polished sections were determined with the MP-SEM-IPS image analysis system. The areal fractions were converted to weight per cent by using the following specific gravities:

silicates 2.8, goethite plus apatite 3.8, pyrite 5.0, pyrrhotite 4.6, tetrahedrite 4.6, barite 4.6, sphalerite 4.1, chalcopyrite 4.3, galena 7.6, and others (mainly arsenopyrite) 4.6. The results show that the sample contains, in wt%, pyrite 88.6, sphalerite 5.3, chalcopyrite 0.3, and galena 0.3 (Table 1). The size distributions for the particles in each fraction were determined with the image analysis system, and the results were combined into size analysis for the sample (Table 2, Fig. 1). The sample is so coarse grained that only 18% of the pyrite is free (Fig. 2, Table 3). The remaining pyrite is in particles that contain inclusions of other minerals, with 66% being in particles that contain more than 90% pyrite and less than 10% other minerals.

Most of the sphalerite, chalcopyrite and galena are unliberated and are largely present as inclusions in pyrite. Almost all the sphalerite occurs in particles that contain less than 90% sphalerite, the chalcopyrite occurs in particles that contain less than 60% chalcopyrite and the galena occurs in particles that contain less than 20% galena (Fig. 2, Table 3). A minor amount of the galena is free.

The large pieces in the sample are equivalent to unbroken ore. Analyses that are required for characterizing an unbroken base metal ore in order to predict how it might behave during mineral beneficiation are:

(1) classification of mode of occurrence of sphalerite, chalcopyrite and galena into:
    (a) occurrence as separate grains;
    (b) occurrence as interstitial fillings among pyrite grains, and
    (c) occurrence as inclusions in pyrite;
(2) determining percentages and size distributions of sphalerite, chalcopyrite and galena in each mode of occurrence;
(3) determining size distributions of pyrite.

The separate grains of sphalerite, chalcopyrite and galena would be liberated when the ore has been ground fine enough to release them. Their size distribution is therefore needed to indicate the grind to liberate them. The minerals occurring among pyrite interstices would be liberated when the ore has been ground fine enough to separate the pyrite grains. The size distribution of pyrite is needed to determine the grind required to release interstitial material. Minerals occurring as inclusions in pyrite would be liberated only when the pyrite grains have been broken to a size

that will release the inclusions. Size distributions of the inclusions in pyrite are necessary to determine this grind.

Some of the above-noted analyses were not carried out because of lack of time and because the analyses were not requested. Nevertheless, size analyses were performed for the sphalerite, chalcopyrite, galena and pyrite grains in large particles (unbroken ore). The sizes of sphalerite, chalcopyrite and galena were determined by measuring chord intercepts across the grains. The sizes of pyrite were determined by reconstructing pyrite grain boundaries, measuring areas of pyrite grains, and assuming that the measured area represents a square. The equivalent edge lengths were calculated from the measured areas of the assumed squares and were designated as the pyrite grain diameters. The grain boundary reconstruction technique was used for pyrite because pyrite grains occur in pyrite masses (Fig. 3). It has been shown by Petruk and Smith (in prep.) that if the pyrite grain boundary is discernible in polished sections, it represents a zone of weakness that will rupture during grinding before the pyrite grains fracture. The rupturing will release grains that occur among pyrite interstices. The size distribution data (Fig. 4 and 5 and Table 4) indicate a bimodal distribution for pyrite grains that compose the pyrite masses: 33% are larger than 37 μm and 67% are smaller. The smaller grains, most of which range from 13 to 37 μm, contain sphalerite, chalcopyrite and galena in interstices, whereas the larger grains do not. Therefore the ore must be ground to at least 80% minus 30 μm to begin liberating interstitial material (about 50% would be liberated at this grind), and to about 80% minus 13 μm to liberate most of the interstitial material. Investigations made by the author on other base metal ores indicate that most ores grind readily to a size that corresponds to the size distribution of pyrite grains (determined by reconstructing grain boundaries), but grinding to finer sizes requires much more energy (Petruk and Smith, in prep.)

Size distribution data show that the sphalerite, chalcopyrite and galena are finer grained than pyrite, which suggests that most of these minerals occur as interstitial fillings and inclusion in pyrite, although a small amount may be present as separate grains. This indicates that about 50% of each mineral might be liberated when the ore is ground to about 80% minus 30 μm, and about 60-80% could be recovered depending upon concentrate

grade and recovery of slimes. The liberation and consequent recovery would be significantly lower if a large proportion of the mineral occurs as inclusions in pyrite.

LSA-03 copper flotation tailing

One polished section was prepared from the sample and was analyzed with the MP-SEM-IPS image analysis system to identify the minerals and to determine quantities, liberations and size distributions of the minerals. Mineral quantities were determined by measuring areal fractions and converting the data to wt% using the same specific gravities as for sample LSA-01. The results show that the sample contains, in wt%, pyrite 73.3, chalcopyrite 4.7, sphalerite 0.5, galena 0.1 and tetrahedrite 0.1 (Table 1).

Size analysis data show that 87 wt% of the particles in the sample are smaller than 26 µm. Hence, the sample was ground to a slightly finer grain size than the minimum grind for separating pyrite grains, as determined by the analysis of sample LSA-01.

Liberation analysis (see Fig. 6 and Tables 5a and 5b)

pyrite
- 67.3% is free
- 22% is in particles that contain more than 90% pyrite and less than 10% other minerals
- 11% is in particles that contain less than 90% pyrite.

chalcopyrite
- 3.4% is free
- 67.9% is in particles that contain 60-99.9% chalcopyrite. (The chalcopyrite grains in these particles range from 3.25 to 37 µm in diameter, and hence may be recoverable)
- 28.7% is in particles that contain less than 50% chalcopyrite. Such particles are normally lost to tailings
- 71.3% of chalcopyrite may be recoverable

sphalerite
- 26.3% is free, but 16.7% is in grains smaller than 3.25 µm (slimes), hence only 9.6% may be recoverable
- 13.9% is in particles that contain more than 90% sphalerite (may be recoverable)
- 46.1% is in particles that contain less than 90% sphalerite (is unrecoverable)

galena - The sample contains only 0.1 wt% galena but 69.7% of it is in free grains that are smaller than 6.5 µm in diameter.

LSA-02 (pyrite sinter)

The sample was screened into plus 424 µm (+35 mesh), 424-53 µm (35-270 mesh) and minus 53 µm (-270 mesh) fractions because the size range of the particles is too wide to analyze everything in one polished section. The weight per cent of the fractions was: +424 µm 72.8, 424-53 µm 19.9, and -53 µm 7.3. THe fractions were analyzed with the MP-SEM-IPS image analysis system and the data were combined by computer by allocating the contribution of each fraction to the sample on the basis of weight per cent. Size analysis data for the particles are included in Table 2 and Figure 1.

The minerals were identified with the energy dispersive X-ray analyzer (EDXA), with the microprobe, and by X-ray diffraction (XRD). The minerals are oxides, silicates, sulphides, sulphates, and metal. The oxides are hematite, magnetite, zincite and rutile; the silicates are quartz, orthoclase, plagioclase, biotite, and a CaFeAl silicate which is probably a pyroxene; the sulphides are sphalerite, pyrite, pyrrhotite and chalcopyrite; the sulphates are barite and Zn-Cu-Fe sulphates, and the metal is lead. Mineral quantities were determined with the image analyzer (Table 6), but the hematite and magnetite occur as such porous material that accurate analysis is impossible. The data, therefore, are only semi-quantitative.

Hematite is the main mineral in the sample. Peak counts by XRD, for the minus 53 µm fraction, indicate that a significant amount of magnetite is present (Fig. 7). The hematite could not be differentiated from magnetite in the backscattered electron image (BSE) because individual hematite and magnetite grains are smaller than 1 µm and the hematite-magnetite material (Fig. 8a and 8b) is so porous that the grey level in the BSE image seems to reflect porosity on a submicroscopic scale rather than compositional differences. Similarly, most of the magnetite could not be differentiated from hematite with an optical microscope because the grains are so small. Microprobe analyses were performed on eleven grains that appeared massive over an area of at least 5 µm x 5 µm. All analyses gave totals considerably less than 100% (Table 7) presumably because the grains are too porous for full excitation. Most analyses reported small amounts of Si, Al, S, Zn and

Cu. It is interpreted that the Si, Al and S are due to sub-microscopic inclusions of silicates and sulphates, trapped in the porous material, and that high values for Zn and Cu (greater than 0.5%) indicate solid solution in magnetite. Consequently microprobe analyses with high Zn and Cu contents were classed as magnetite and with low Zn and Cu contents as hematite. It is possible that Zn and Cu ferrites are present also.

The pyrite, pyrrhotite, chalcopyrite and sphalerite occur as remnants in the porous hematite-magnetite material (Fig. 8C). Microprobe analyses indicate that both Zn-rich and Zn-poor varieties of sphalerite are present (Fig. 8D). Analysis of the Zn-rich variety gave, in wt%, Zn 63.8, Fe 2.2 and S 32.4, and analysis of the Zn-poor variety gave, in wt%, Zn 41.7, Fe 20.4 Cu 2.0, and S 34.5. It is possible that the Zn-poor variety is reprecipitated sphalerite and has an anomalous composition. On the other hand the copper reported in the analysis could be due to an inclusion of a Cu mineral. A small amount of zincite was found as a border on sphalerite (Fig. 8E).

The Zn-Cu-Fe sulphates occur as spheres. They are most abundant in the minus 53 µm fraction although some are present in the 424-53 µm fraction. EDXA analyses indicate a complete range of compositions between zinc sulphate, copper sulphate and iron sulphate. No microprobe analyses were performed on the phases.

Liberation analyses (Table 8) show that most of the hematite-magnetite occurs in particles that contain more than 80 vol% hematite-magnetite. Similarly, most of the barite is in particles that contain more than 80 vol% barite. The quartz is largely in particles that contain more than 70 vol% quartz, the sphalerite is in particles that contain less than 40% sphalerite (i.e., occurs as inclusions) and the sulphates are in all types of particles. Aluminum-bearing silicates occur as inclusions in the hematite-magnetite.

This study indicates tht the zinc occurs in magnetite, Zn-bearing sulphates and sphalerite, and the copper occurs in magnetite, Cu-bearing sulpahtes and chalcopyrite. Only small proportions of the Zn and Cu occur in the sphalerite and chalcopyrite respectively. The distributions of elements in the sulphates and magnetite cannot be accurately determined. A rough calculation indicates that about equal proportions of zinc occur in the sulphates and magnetite. A similar distribution is indicated for copper

ACKNOWLEDGEMENT

The author gratefully acknowledges R.G. Pinard for help in conducting the image analyses and microprobe analyses. Thanks are extended to P. Carriere for the X-ray diffraction analysis and M. Baulne for preparing polished sections.

REFERENCES

W. Petruk and M.M. Smith (in prep.). Ore characteristics that affect breakage during grinding, in preparation for publication in CIM Bull.

Table 1. Mineral Quantities in Samples LSA-01 and 03

	LSA-01	LSA-03
Pyrite	88.6	73.3
Pyrrhotite	0.8	0.9
Chalcopyrite	0.3	4.7
Sphalerite	5.3	0.5
Galena	0.3	0.1
Tetrahedrite	0.1	0.1
Barite	0.9	0.1
Geothite and apatite	0.4	1.6
Silicate minerals	2.7	17.8
Other (mainly arsenopyrite)	0.6	0.9
Total	100.0	100.0

Table 2. Size Analyses* of Particles in Samples

size µm	LSA-01	LSA-02	LSA-03
3.25	0.5	-	13.8
4.60	0.8	-	22.7
6.50	1.1	-	34.6
9.20	1.7	0.2	49.6
13.0	2.2	0.4	66.2
18.4	2.8	1.0	80.3
26	3.5	2.0	87.0
37	4.5	4.2	92.2
52	4.7	7.3	96.1
74	5.4	8.8	98.0
104	6.1	11.1	100.0
147	7.0	13.8	100.0
208	7.8	16.5	100.0
424	12.1	27.2	100.0
+424	87.9	72.8	0.0

*% smaller than.

Table 3. Percentages of Minerals* in different Classes of Particles

particle class	pyrite	sphalerite	chalcopyrite	galena
0-10	0.1	15.8	44.0	82.6
10-20	0.2	13.1	47.2	7.4
20-30	0.4	12.8	1.4	0.7
30-40	0.6	11.6	0.05	0.9
40-50	0.8	4.9	0.2	0.6
50-60	1.5	8.6	5.7	0.2
60-70	1.1	7.4	0.3	0.3
70-80	3.9	17.1	0.3	0.7
80-90	7.4	7.1	0.05	0.5
90-99.99	66.0	0.7	0.4	0.7
+99.99 (free)	18.0	0.9	0.4	5.4
Total	100.0	100.0	100.0	100.0

*Sample LSA-01

Table 4. Size Distributions* of Minerals in Large Particles from Sample LSA-01

size	pyrite	sphalerite	chalcopyrite	galena
3.25	0.3	6.0	8.4	22.5
4.6	0.7	8.9	10.9	29.0
6.5	1.3	15.0	25.5	38.5
9.2	2.9	24.4	53.5	49.0
13.0	7.0	33.3	67.1	61.2
18.4	18.8	48.4	88.1	72.1
26.0	41.4	62.3	100.0	84.8
37.0	67.8	76.4	100.0	94.1
52.0	81.6	87.3	100.0	99.3
74.0	88.0	95.5	100.0	100.0
104.0	92.0	98.9	100.0	100.0
147.0	96.0	99.5	100.0	100.0
208.0	96.0	99.8	100.0	100.0
+208.0	4.0	0.2	0.0	0.0

*% smaller than.

Table 5a. Data for classification of pyrite and sphalerite in sample LSA-03. These data were used to plot the diagrams shown in Figues 5. the sizes (vertical left column) are sizes of pyrite and sphalerite grains in the particles. The top line defines particle classifications (phase %), and the bottom line is the sum of classifications for grains of all sizes. The right column is the sum of grains sizes for particles of all classifications.

pyrite

	9.99	20.0	30.0	40.0	50.0	60.0	70.0	80.0	90.0	100.0		
3.25	.623E-01	.231E-01	.313E-01	.378E-01	.786E-01	.859E-01	.166	.241	.158	.106E-01	6.64	7.53
4.60	.388E-01	.257E-01	.388E-01	.389E-01	.555E-01	.453E-01	.102	.208	.689	.260	8.32	9.71
6.50	.235E-01	.773E-01	.671E-01	.229E-01	.688E-01	.844E-01	.181	.287	.674	1.36	12.0	14.8
9.19	.255E-01	.236E-01	.221E-01	.516E-01	.129	.195	.564E-01	.147	.811	3.48	13.9	18.7
13.0	.485E-01	.849E-01	.799E-01	.196	.456E-01	.138	.229	.257	.619	4.49	14.7	20.9
18.4	0.00	0.00	0.00	0.00	0.00	.124	.175	.804E-01	.689	6.25	7.51	14.8
26.0	0.00	0.00	0.00	.285	0.00	.299	.218	.223	0.00	1.79	3.47	6.28
36.8	0.00	0.00	0.00	0.00	0.00	.525	0.00	0.00	.384	1.76	.683	3.35
52.0	0.00	0.00	0.00	0.00	0.00	0.00	0.00	0.00	0.00	1.24	0.00	1.24
73.5	0.00	0.00	0.00	0.00	0.00	0.00	0.00	0.00	1.33	1.36	0.00	2.69
104.	0.00	0.00	0.00	0.00	0.00	0.00	0.00	0.00	0.00	0.00	0.00	0.00
147.	0.00	0.00	0.00	0.00	0.00	0.00	0.00	0.00	0.00	0.00	0.00	0.00
208.	0.00	0.00	0.00	0.00	0.00	0.00	0.00	0.00	0.00	0.00	0.00	0.00
	0.00	0.00	0.00	0.00	0.00	0.00	0.00	0.00	0.00	0.00	0.00	0.00
	.187	.215	.251	.633	.377	1.46	1.05	1.44	5.26	22.0	67.3	100.0

sphalerite

	9.99	20.0	30.0	40.0	50.0	60.0	70.0	80.0	90.0	100.0		
3.25	11.3	4.77	1.82	3.13	1.07	.820	.281	0.00	.886E-01	.287	16.7	40.2
4.60	3.64	3.09	2.06	1.32	.657	0.00	.753	0.00	1.71	0.00	2.38	16.3
6.50	9.90	4.43	0.00	0.00	0.00	0.00	0.00	0.00	0.00	0.00	0.00	14.3
9.19	0.00	0.00	0.00	0.00	0.00	0.00	0.00	0.00	0.00	0.00	6.60	15.5
13.0	0.00	0.00	0.00	0.00	0.00	0.00	0.00	0.00	0.00	0.00	0.00	0.00
18.4	0.00	0.00	0.00	0.00	0.00	0.00	0.00	0.00	0.00	13.7	0.00	13.7
26.0	0.00	0.00	0.00	0.00	0.00	0.00	0.00	0.00	0.00	0.00	0.00	0.00
36.8	0.00	0.00	0.00	0.00	0.00	0.00	0.00	0.00	0.00	0.00	0.00	0.00
52.0	0.00	0.00	0.00	0.00	0.00	0.00	0.00	0.00	0.00	0.00	0.00	0.00
73.5	0.00	0.00	0.00	0.00	0.00	0.00	0.00	0.00	0.00	0.00	0.00	0.00
104.	0.00	0.00	0.00	0.00	0.00	0.00	0.00	0.00	0.00	0.00	0.00	0.00
147.	0.00	0.00	0.00	0.00	0.00	0.00	0.00	0.00	0.00	0.00	0.00	0.00
208.	0.00	0.00	0.00	0.00	0.00	0.00	0.00	0.00	0.00	0.00	0.00	0.00
	33.0	12.3	3.89	4.45	1.73	.820	1.03	0.00	1.79	13.9	26.3	100.

Table 5b. Data for classification of chalcopyrite and galena in sample LSA-03. These data were used to plot the diagrams shown in Figure 5. The sizes (left column) are sizes of chalcopyrite and galena grains in the particles. The top line defines particle classifications (phase %), and the bottom line is the sum of classifications for grains of all sizes. The right column is the sum of grain sizes for particles of all classifications.

chalcopyrite

	9.99	20.0	30.0	40.0	50.0	60.0	70.0	80.0	90.0	100.0	
1.19		.674	.185	.196	.559E-01	.897	.867E-01	.185	.917E-01	.123	1.55	4.47
3.25												
	.855	0.00	.179	.777	0.00	.759E-01	.666	.265	.257	.493	.178	3.74
4.60												
	.397	1.24	0.00	.384	.439	.335	.479	.816	.852	.489	1.06	6.50
6.50												
	0.00	.383	.650	1.45	.856	.268	0.00	.759	1.80	2.61	.579	9.35
9.19												
	0.00	.782	0.00	2.86	2.00	0.00	.683	.742	1.23	7.41	0.00	15.0
13.0												
	0.00	0.00	0.00	1.56	0.00	0.00	4.54	1.35	3.79	8.00	0.00	19.2
18.4												
	0.00	2.48	0.00	0.00	3.26	0.00	0.00	4.66	0.00	5.84	0.00	15.6
26.0												
	0.00	0.00	0.00	0.00	5.79	0.00	6.38	0.00	4.67	0.00	0.00	16.8
36.8												
	0.00	0.00	0.00	0.00	0.00	0.00	0.00	0.00	0.00	9.36	0.00	9.36
52.0												
	0.00	0.00	0.00	0.00	0.00	0.00	0.00	0.00	0.00	0.00	0.00	0.00
73.5												
	0.00	0.00	0.00	0.00	0.00	0.00	0.00	0.00	0.00	0.00	0.00	0.00
104.												
	0.00	0.00	0.00	0.00	0.00	0.00	0.00	0.00	0.00	0.00	0.00	0.00
147.												
	0.00	0.00	0.00	0.00	0.00	0.00	0.00	0.00	0.00	0.00	0.00	0.00
208.												
	0.00	0.00	0.00	0.00	0.00	0.00	0.00	0.00	0.00	0.00	0.00	0.00
	2.44	5.41	1.81	6.56	12.4	.885	12.8	8.12	12.7	34.3	3.38	100.

Galena

variable x: PER CENT
variable x: PHASEX
variable y: DIA(MIC)

	9.99	20.0	30.0	40.0	50.0	60.0	70.0	80.0	90.0	100.0		
	8.26	1.74	1.86	.290	.813	0.25	0.00	1.97	2.96	0.00	16.1	35.2
3.25												
	5.34	0.00	0.00	0.00	0.00	0.00	0.00	4.76	0.00	0.00	34.2	44.3
4.60												
	0.00	0.00	0.00	0.00	0.00	0.00	0.00	0.00	0.00	0.00	19.5	19.5
6.50												
	0.00	0.00	0.00	0.00	0.00	0.00	0.00	0.00	0.00	0.00	0.00	0.00
9.19												
	0.00	0.00	0.00	0.00	0.00	0.00	0.00	0.00	0.00	0.00	0.00	0.00
13.0												
	0.00	0.00	0.00	0.00	0.00	0.00	0.00	0.00	0.00	0.00	0.00	0.00
18.4												
	0.00	0.00	0.00	0.00	0.00	0.00	0.00	0.00	0.00	0.00	0.00	0.00
26.0												
	0.00	0.00	0.00	0.00	0.00	0.00	0.00	0.00	0.00	0.00	0.00	0.00
36.8												
	0.00	0.00	0.00	0.00	0.00	0.00	0.00	0.00	0.00	0.00	0.00	0.00
52.0												
	0.00	0.00	0.00	0.00	0.00	0.00	0.00	0.00	0.00	0.00	0.00	0.00
73.5												
	0.00	0.00	0.00	0.00	0.00	0.00	0.00	0.00	0.00	0.00	0.00	0.00
104.												
	0.00	0.00	0.00	0.00	0.00	0.00	0.00	0.00	0.00	0.00	0.00	0.00
147.												
	0.00	0.00	0.00	0.00	0.00	0.00	0.00	0.00	0.00	0.00	0.00	0.00
208.												
	0.00	0.00	0.00	0.00	0.00	0.00	0.00	0.00	0.00	0.00	0.00	0.00
	7.61	1.74	1.86	.290	.813	0.25	0.00	6.74	2.96	0.00	69.7	100.

Table 6. Mineral Quantities in Sample LSA-02

Mineral	Vol%
hematite and magnetite	90.1
quartz	3.0
other silicates	1.7
Zn-Cu-Fe sulphates	1.4
sphalerite	0.1
pyrite	trace.
pyrrhotite	trace.
chalcopyrite	trace.
zincite	trace.
lead	trace.
barite	3.7
Total	100.0

Table 7. Microprobe Analyses for Hematite and Magnetite

oxide or element	hematite			magnetite		
	grain 1	grain 2	grain 3	grain 1	grain 2	grain 3
Fe_2O_3	90.8	88.3	82.2	-	-	-
Fe_3O_4	-	-	-	92.2	85.5	75.6
CuO	-	0.3	-	0.8	0.5	0.8
ZnO	-	0.3	0.4	1.5	3.2	1.8
SiO_2	-	0.2	0.2	1.5	0.6	3.8
Al_2O_3	-	-	-	0.7	0.6	1.5
S	0.2	0.1	0.4	0.4	0.7	0.5
Total	91.0	89.3	83.2	97.1	91.1	84.0

Table 8. Percentages of Mineral in Different Classes of Particles for Sample LSA-02

particle class	hematite-magnetite	barite	quartz	sphalerite	Zn-Cu-Fe sulphates
0-10	0.0	1.0	11.4	58.0	13.7
10-20	0.6	31.7	3.6	14.8	10.1
20-30	0.2	0.1	0.6	6.5	6.5
30-40	0.1	0.0	3.6	14.6	6.5
40-50	0.3	0.6	1.5	3.0	2.9
50-60	0.0	1.6	1.2	0.0	11.6
60-70	0.3	0.1	2.0	0.0	11.3
70-80	0.3	0.0	23.4	0.4	2.1
80-90	11.3	61.0	3.4	1.1	14.4
90-99.99	72.8	2.3	13.7	0.0	10.0
+99.99(free)	14.1	1.6	35.6	0.8	10.9

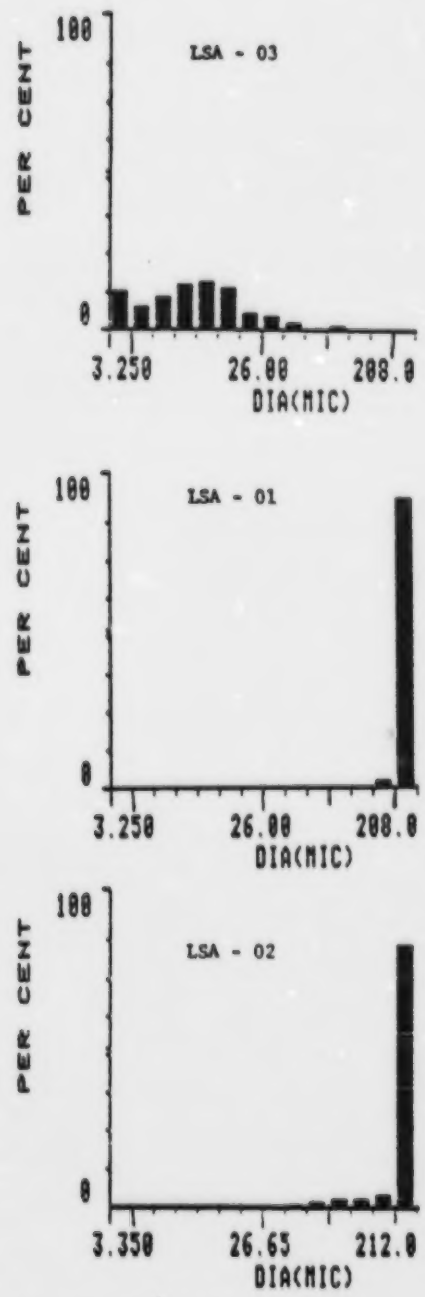

Fig. 1. Histograms showing size distributions of samples. The size ranges of the particles are 0-3.25, 3.25-4.6, 4.6-6.5, 6.5-9.2, 9.2-13, 13--18.5, 18.5-26, 26-37, 37-52, 52-74, 74-104, 104-147, 147-208, and +208 μm in diameter. The bar heights represent the proportion of particles within size range.

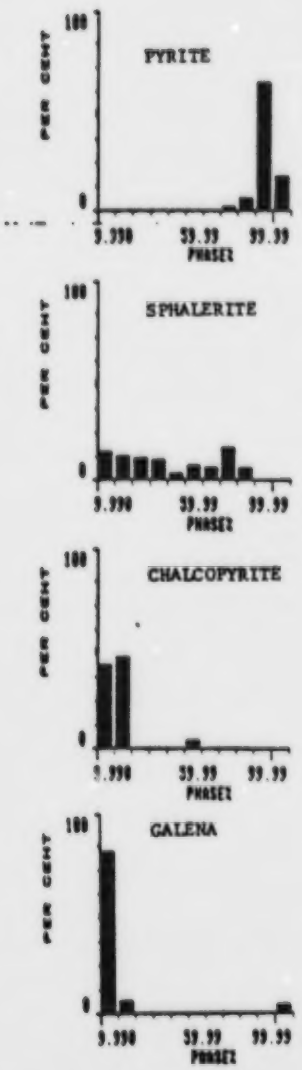

Fig. 2. Classification of pyrite, sphalerite, chalcopyrite and galena in Sample LSA-01, as volume % of mineral in particle. The classification steps are 0-9.99, 9.99-19.99, 19.99-29.99, 29.99-39.99, 39.99-49.99, 49.99-59.99, 59.99-69.99, 69.99-79.99, 79.99-89.99, 89.99-99.99 and + 99.99 vol% of mineral in particle. The heights of the bars refer to proportion of mineral that occurs in particular type of particle. The particle size was disregarded in this classification.

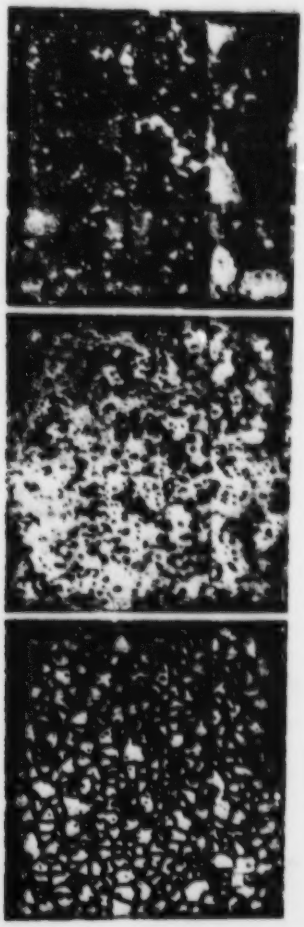

Fig. 3. Diagrams to show grain boundary reconstruction technique.

Top diagram = BSE image transferred to image analyzer, pyrite=grey, sphalerite+galena = white, silicates = black;

Middle diagram = binary image of pyrite. The areas occupied by sphalerite and silicates are black, and dots indicate incipient grain boundaries;

Bottom diagram = reconstructed boundaries for pyrite grains in massive pyrite.

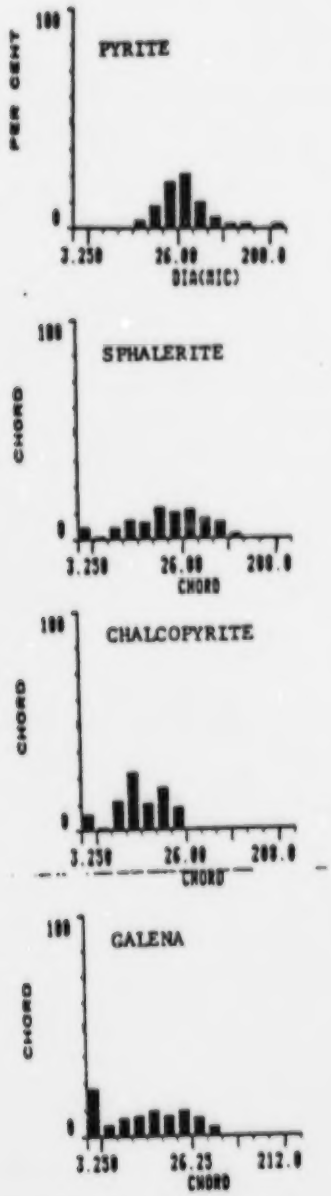

Fig. 4. Size distributions for pyrite, sphalerite, chalcopyrite and galena in large pieces from sample LSA-01. The pyrite sizes are for grains in pyrite masses as determined by a grain boundary reconstruction technique. The sphalerite, chalcopyrite and galena grain sizes were determined by measuring lengths across grains. The steps along the base of the diagram are size of grains and are 3.25, 4.6, 6.5, 9.2, 13.0, 18.4 26, 37, 52, 74, 104, 147, and 208 μm. The bar heights refer to per cent of mineral in each size range.

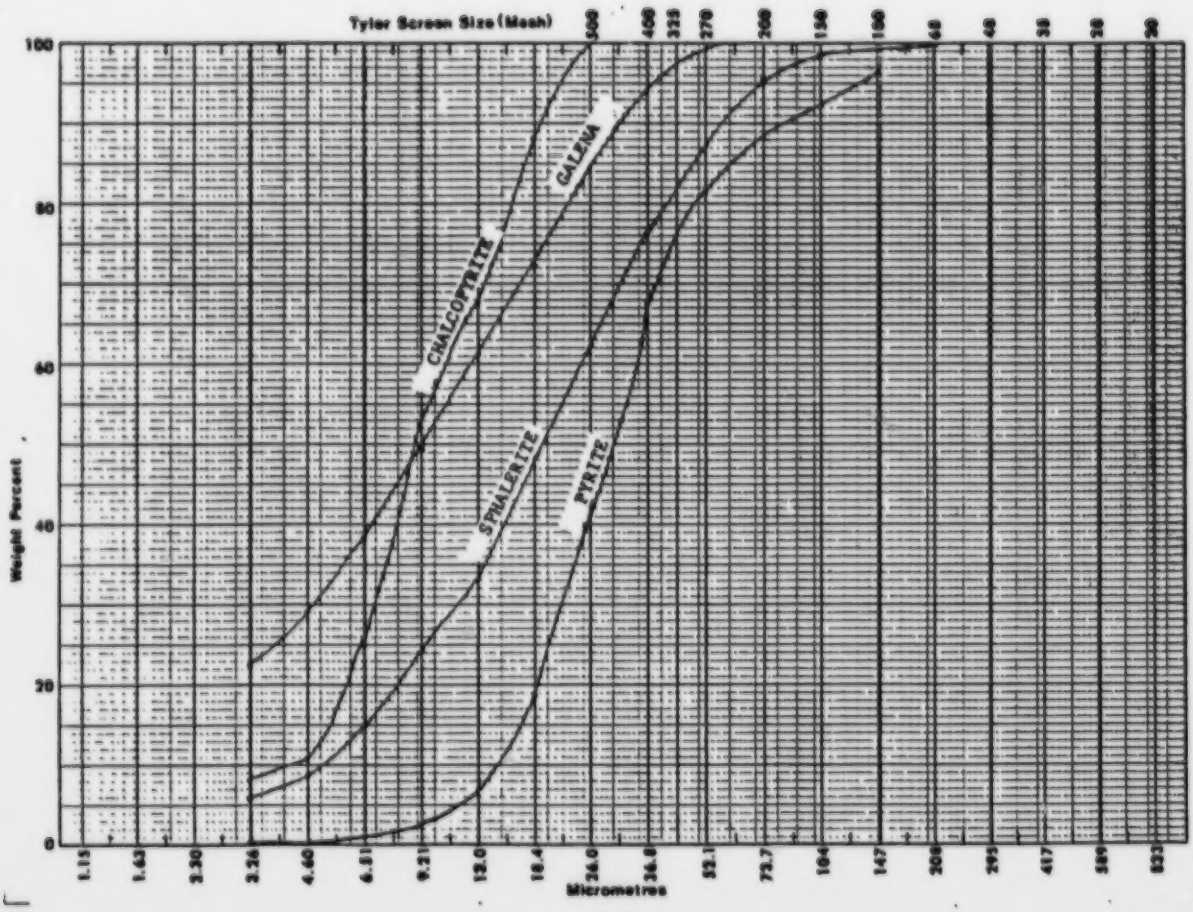

Fig. 5. Size distributions for the pyrite, sphalerite, chalcopyrite and galena referred to in Figure 4, but plotted as cumulative % passing or % smaller than.

Fig. 6. Diagrams showing the liberation characteristics of chalcopyrite, sphalerite, galena and pyrite in Sample LSA-03. The left diagrams show the classification of particles containing the minerals. The classification (phase %) is for particles containing 0-10 (9.99), 10- 20, 20-30, 30-40, 40-50, 50-60 (59.99), 60-70, 70-80, 80-90, 90-99.99 (free) and 100 (free) vol% of the respective minerals. The heights of the bars represent the proportions of mineral in each class of particle. The middle diagrams show the size distribution of mineral grains in the particles. The size steps are -3.25, 3.25, 4.6, 6.5, 9.25, 13, 18.5, 26, 37, 52, 74, 104, 147, 208 and plus 208. The 3D diagrams are combinations of the classifications and size distributions. The front of the diagrams corresponds to the classification with the extreme left line being for the 0-10 vol% class, and the extreme right for the 100 vol% class. The size is along the side of the diagram, with the -3.25 μm grains being along the front line, and the plus 208 μm grains along the back line.

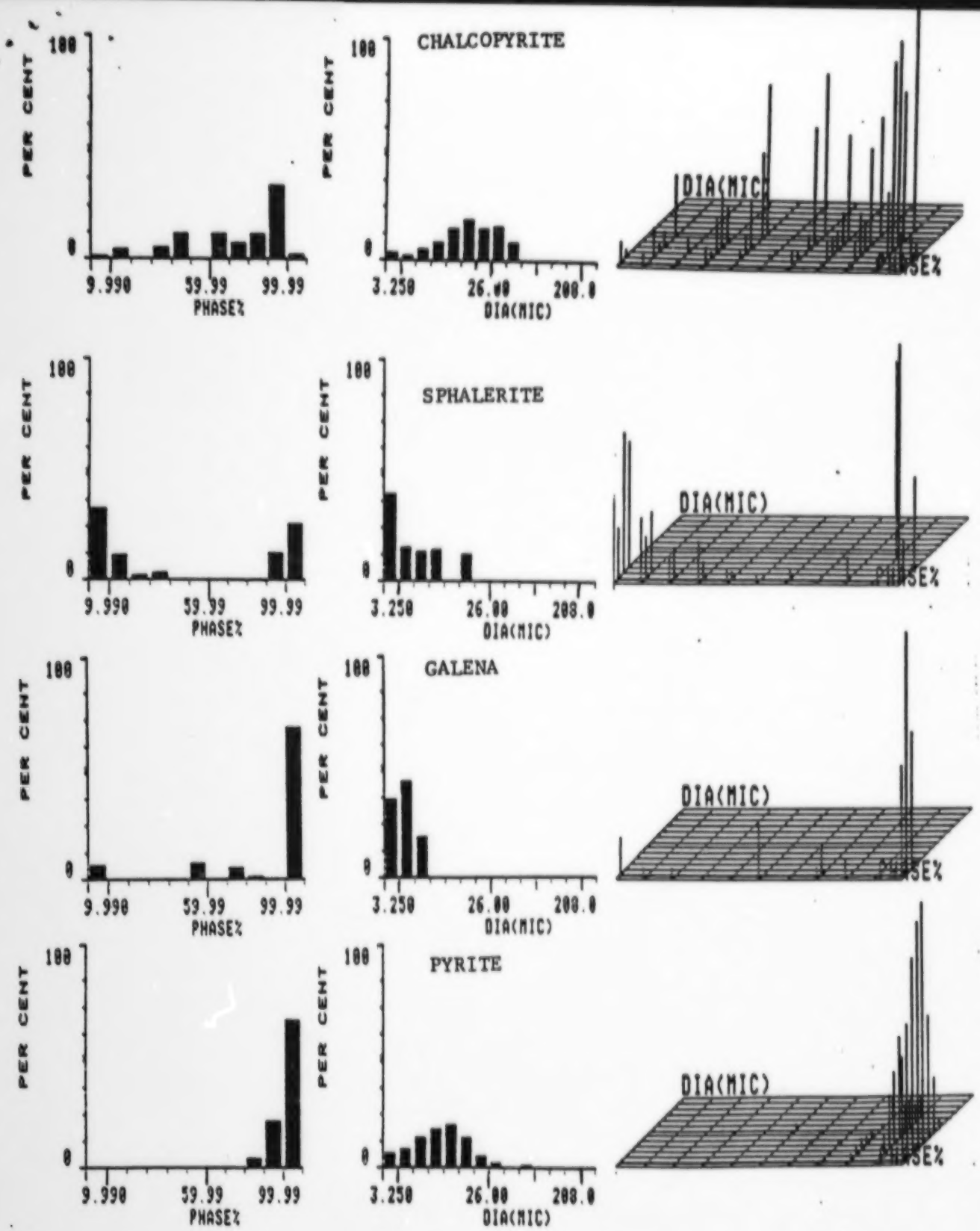
CHALCOPYRITE
SPHALERITE
GALENA
PYRITE
PER CENT
100
0
9.990
59.99
99.99
PHASE%
3.250
26.00
208.0
DIA(MIC)

Fig. 6

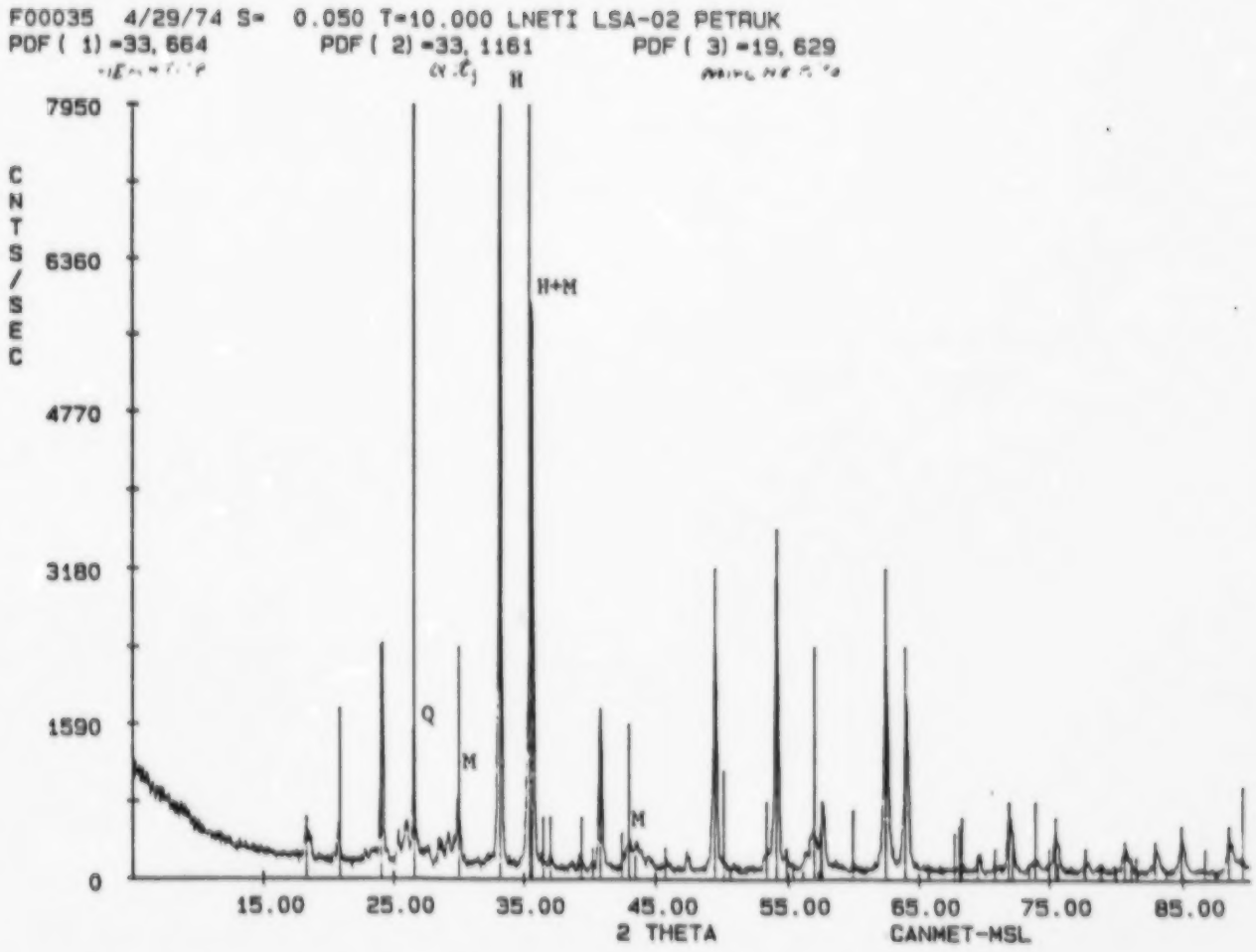

Fig. 7. XRD tracing for -53 μm fraction of sample LSA-02. The tracing shows peak heights for hematite (H), magnetite (M) and quartz (Q). The sample contains 2.2 vol% quartz.

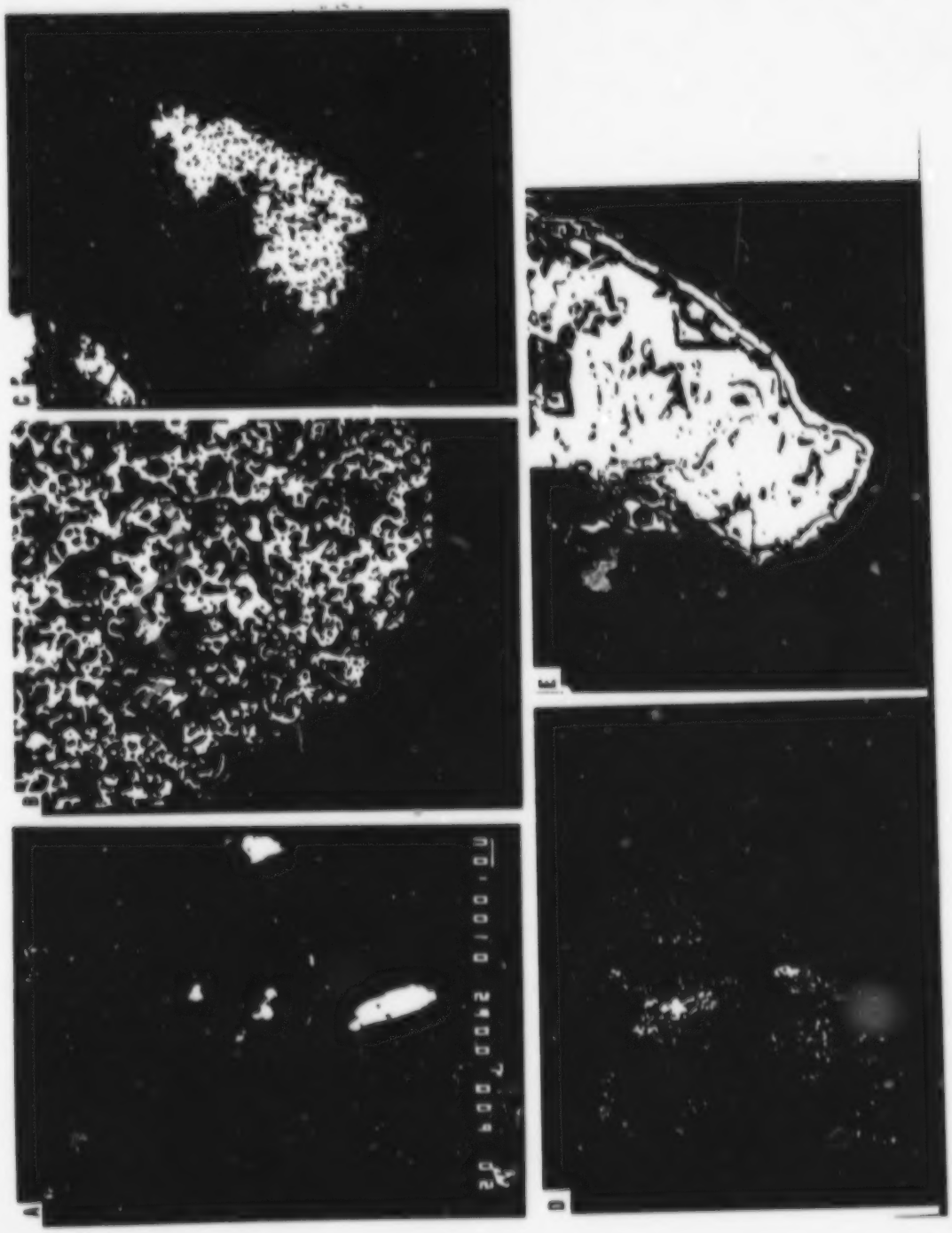

Fig. 8. BSE photomicrographs of sample LSA-02. (A) General field showing hematite-magnetite (grey) and barite (white); (B) high magnification showing porosity of hematite-magnetite; (C) remnant of pyrite and chalcopyrite (white) in magnetite-hematite; (D) Zn-rich sphalerite (light grey) in Zn-poor sphalerite (grey); (E) border of zincite (light grey) on sphalerite (white).